Simulation and measurement of the resonant Schottky pickup*

ZANG Yong-Dong(臧永东)[1,2;1)] WU Jun-Xia(武军霞)[1] ZHAO Tie-Cheng(赵铁成)[1]
ZHANG Sheng-Hu(张生虎)[1] MAO Rui-Shi(毛瑞士)[1] XU Hu-Shan(徐瑚珊)[1]
SUN Zhi-Yu(孙志宇)[1] MA Xin-Wen(马新文)[1] TU Xiao-Lin(涂小林)[1,2]
XIAO Guo-Qing(肖国青)[1] F. Nolden[3] P. Hülsmann[3] Yu. A. Litvinov[3]
C. Peschke[3] P. Petri[3] M. S. Sanjari[3] M. Steck[3]

[1] Institute of Modern Physics, Chinese Academy of Sciences, Lanzhou 730000, China
[2] Graduate University of Chinese Academy of Sciences, Beijing 100049, China
[3] Gesellschaft für Schwerionenforschung, Darmstadt, Germany

Abstract: A resonant Schottky pickup with high sensitivity, built by GSI, will be used for nuclear mass and lifetime measurement at CSRe. The basic concepts of Schottky noise signals, a brief introduction of the geometry of the detector, the transient response of the detector, and MAFIA simulated and perturbation measured results of characteristics are presented in this paper. The resonant frequency of the pickup is about 243 MHz and can be slightly changed at a range of 3 MHz. The unloaded quality factor is about 1072 and the shunt impedance is 76 kΩ. The measured results of the characteristics are in agreement with the MAFIA simulations.

Key words: resonant Schottky pickup, Schottky signal, characteristics of the eigenmode TM_{010}

PACS: 82.80.Nj **DOI:** 10.1088/1674-1137/35/12/008

1 Introduction

Nuclear physics and astrophysics studies on highly charged ions benefit from accelerators with storage rings, where exotic nuclei produced with small yields can be efficiently stored [1, 2]. The measured high accuracy data of masses and lifetimes make valuable contributions to the understanding of the pathways of stellar nucleosynthesis processes and to the exploration of the limits of nuclear stability at both the proton and the neutron drip line [3].

There are two complementary methods of mass measurement, isochronous mass spectrometry for short-lived [4] and Schottky mass spectrometry for long-lived exotic nuclei. In Schottky spectrometry the velocity spread of the ions stored in the ring is reduced by electron cooling. Non-destructive methods based on frequency analysis of Schottky noise power are usually used for in-flight measurement. The sensitivity of such detection systems is of great importance since the number of stored ions is small. A resonant Schottky pickup with high sensitivity, built by GSI [5], will be applied at CSRe to study the nuclear properties of highly charged ions using time-resolved Schottky mass spectrometry and lifetime measurement. The basic concepts of Schottky noise, and the simulation and measurement results of the characteristics of the detector will be presented.

2 Longitudinal Schottky signal

Since the resonant Schottky pickup cannot be applicable to measure the transverse Schottky signal, only the longitudinal signal basic is described. A single particle of charge qe circulating in the storage ring with a constant revolution time T_{r} induces a series of δ function pulses onto the pickup placed somewhere around the ring with its initial passage time t_0. The current created is

Received 2 March 2011
* Supported by National Natural Science Foundation of China (10925526, 11079044)
1) E-mail: zangyongdong@impcas.ac.cn

$$I_{\mathrm{s}}(t)=qe\sum_{m}\delta(t-t_0-mT_{\mathrm{r}}). \tag{1}$$

The frequency spectrum, i.e. the Fourier transform of this current is an infinite train of δ functions as well,

$$\tilde{I}_{\mathrm{s}}(f)=qef_{\mathrm{r}}\sum_{m}\delta(f-mf_{\mathrm{r}})\mathrm{e}^{-j2\pi ft_0}, \tag{2}$$

where $f_{\mathrm{r}}=1/T_{\mathrm{r}}$, f_{r} is the revolution frequency.

If considering a costing ion beam, i.e. an ion beam of N particles randomly spread along the ion orbit in the ring, the initial passage time of the individual particle labeled i $t_{0,i}$ is randomly distributed. The total signal of the costing ion beam is the sum over all particles

$$I_N(\mathrm{t})=qe\sum_{i=1}^{N}\sum_{m}\delta(t-t_{0,i}-mT_{\mathrm{r},i}), \tag{3}$$

$T_{\mathrm{r},i}$ is the revolution time of the particle labeled i. The Fourier transform is

$$\tilde{I}_N(f)=qe\sum_{i=1}^{N}\sum_{m}f_{\mathrm{r},i}\delta(f-mf_{\mathrm{r},i})\mathrm{e}^{-j2\pi ft_{0,i}}, \tag{4}$$

where $f_{\mathrm{r},i}=1/T_{\mathrm{r},i}$. The spectrum consists of peaks at each harmonic of the revolution frequency $f_{\mathrm{r},i}$ with a random phase. The expectation value of $\tilde{I}_N(f)$ vanishes due to the random phase. However its power spectrum can be observed as a Schottky band at a given harmonic of the mean revolution frequency f_{r} of the constituent particles, the width of the Schottky band is the product of the harmonic number and the revolution frequency distribution δf which corresponds to the velocity distribution of the constituent particles. The best choice for the harmonic number m is the one that satisfies $mf_{\mathrm{r}}=f_0$, where f_0 is the resonant frequency of the resonant Schottky pickup. The relative revolution frequency spread is proportional to the relative momentum spread of the ion beam

$$\frac{\delta f}{f_{\mathrm{r}}}=\eta\frac{\delta p}{p_0} \tag{5}$$

with the frequency dispersion $\eta=\gamma^{-2}-\alpha_{\mathrm{p}}$, where p_0 is the mean momentum, δp is the momentum spread, γ is the Lorentz factor, and α_{p} is the momentum compaction factor of the ring lattice. α_{p} is related to the transition point γ_{t} by $\alpha_{\mathrm{p}}=\gamma_{\mathrm{t}}^{-2}$. It is possible to infer from the power spectrum the momentum spread of the ion beam. It is sufficient to measure the spectrum at a given harmonic, but a higher harmonic is always chosen in order to get good frequency resolution. With a calibrating system, i.e. beam current transformer, the number of particles can also be deduced, which is the basis of nuclear lifetime measurement [5]. For the mass measurement, the nuclide mass can be evaluated with reference nuclides from the power spectrum [6].

3 Resonant Schottky pickup

The resonant Schottky pickup is a pillbox-like resonator, resonating at about 243 MHz. The pickup is composed of a ceramic gap with a beam pipe on both ends and an air-filled resonator with holes on both end walls to tightly connect the beam pipe with the ceramic gap. The ceramic gap protects the vacuum in the beam pipe from the outside resonator, and the beam couples energy into the resonator through the ceramic gap. The outer diameter of the resonator is 600 mm and the inside length is 90 mm. The inside surface of the resonator is plated with copper of a thickness of about 50 μm in order to reduce the ohm loss and therefore enhance the unloaded quality factor Q. Furthermore the resonator is split into two identical halves, the half-cylinders could be removed when the detector is not needed, thereby shortening the ceramic gap, the high current experiments at the CSRe are not affected. An additional advantage is that the radial split will suppress excitation of the high eigenmodes which have an azimuthal surface current component but do not influence the desired Q factor and shunt impedance since the first eigenmode TM_{010} has only surface current components in the radial and longitudinal directions. The detector is equipped with two moveable copper plungers for tuning its resonant frequency at a range of 3 MHz, which is sufficient to cover the whole acceptance of the storage ring CSRe. A well-matched coupling loop is used for the extraction of beam-induced energy.

The output loop of the resonant pickup is carefully designed to be matched with load impedance $Z_{\mathrm{L}}=50\ \Omega$ at the resonance frequency. The ratio of the output voltage to the beam current, $Z_{\mathrm{P}}=V(t)/I(t)$, is called the longitudinal transfer impedance. Therefore the signal power from the pickup into the external load impedance Z_{L} is

$$P_{\mathrm{o}}=\langle I^2(t)\rangle\,Z_{\mathrm{P}}^2/Z_{\mathrm{L}}. \tag{6}$$

Z_{P} is related to the shunt impedance R_{s} and transit time factor Λ with [7]

$$Z_{\mathrm{P}}=\sqrt{Z_{\mathrm{L}}R_{\mathrm{s}}\Lambda^2}/2, \tag{7}$$

thus P_{o} can be expressed as

$$P_{\mathrm{o}}=\langle I^2(t)\rangle\,R_{\mathrm{s}}\Lambda^2/4. \tag{8}$$

When a beam passes through the resonant pickup, it excites the cavity modes due to its electromagnetic fields. The self-induced electromagnetic fields act back on the beam, causing it to lose energy. The ratio of the beam energy loss (expressed as a voltage) to the beam current is defined as the longitudinal beam impedance. The longitudinal beam impedance of the resonant pickup in an equivalent circuit can be modeled as a parallel RLC circuit connected to the external circuit via an impedance matching device such as a transformer [8], shown in Fig. 1.

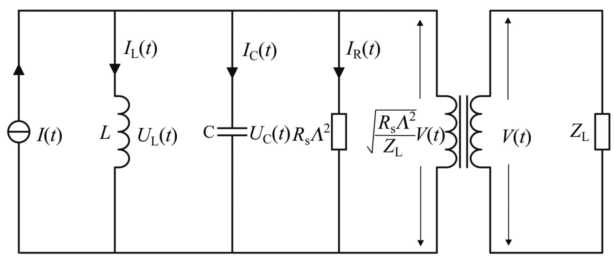

Fig. 1. Equivalent circuit of the resonant pickup. $I(t)$ is the beam current, $I_{\rm L}(t)$, $I_{\rm C}(t)$, $I_{\rm R}(t)$ are the transient currents of the inductor, capacitor and resistor respectively, and $U_{\rm L}(t)$, $U_{\rm C}(t)$ are the corresponding voltages. The voltage ratio of the transformer is $\sqrt{\frac{R_{\rm s}\Lambda^2}{Z_{\rm L}}}V(t):V(t)$.

The existence of the matched external load decreases the impedance, $R_{\rm s}\Lambda^2$, of the resonant pickup by half. The longitudinal beam impedance is written as [9]

$$Z(f)=\frac{R_{\rm s}\Lambda^2}{2}\left(1+\frac{jQf}{f_0}-\frac{jQf_0}{f}\right)^{-1}. \qquad (9)$$

The time domain response to a single excitation $I(t)=qe\delta(t)$ is simply characterized by the following formula with the initial condition $U_{\rm C}(0-)=0$ and $I_{\rm L}(0-)=0$.

$$\frac{{\rm d}^2I_{\rm L}}{{\rm d}t^2}+\frac{2\pi f_0}{Q}\frac{{\rm d}I_{\rm L}}{{\rm d}t}+4\pi^2f_0^2I_L=4\pi^2f_0^2qe\delta(t). \qquad (10)$$

When a charged particle passes through the resonator, the capacitor C is suddenly charged by the current $qe\delta(t)$. The transient voltage $U_{\rm C}(0+)$ is $\pi f_0R_s\Lambda^2/Q$. Directly after the particle has left the resonant pickup, the RLC circuit starts to oscillate with the condition $U_{\rm C}(0+)=\pi qef_0R_{\rm s}\Lambda^2/Q$ and $i_{\rm L}(0+)=0$. The underdamped response is simply derived from the characteristic equation with $Q\gg 1/2$,

$$I_{\rm L}(t)=2\pi\frac{qef_0^2}{f_{\rm d}}{\rm e}^{-t/\tau}\sin(2\pi f_{\rm d}t), \qquad (11)$$

where

$$f_{\rm d}=f_0\sqrt{1-\frac{1}{4Q^2}}$$

and $\tau=\frac{Q}{\pi f_0}$. Therefore the transient voltage is directly calculated from $U_{\rm L}(t)=L\frac{{\rm d}I_{\rm L}}{{\rm d}t}$, by inserting the value of $I_{\rm L}$,

$$\begin{aligned}U_{\rm L}(t) &= \pi qe\frac{R_{\rm s}\Lambda^2}{Q}f_0{\rm e}^{-t/\tau}\cos(2\pi f_{\rm d}t)\\ &\quad -qe\frac{R_{\rm s}\Lambda^2}{2Q}\frac{1}{\tau f_{\rm d}}f_0{\rm e}^{-t/\tau}\sin(2\pi f_{\rm d}t). \qquad (12)\end{aligned}$$

For a high Q resonator one gets a good approximation with $f_{\rm d}\approx f_0$ and $2\pi\tau f_{\rm d}\gg 1$, therefore

$$U_{\rm L}(t)\approx\pi qe\frac{R_{\rm s}\Lambda^2}{Q}f_0{\rm e}^{-t/\tau}\cos(2\pi f_0t). \qquad (13)$$

This leads to an output voltage

$$\begin{aligned}V(t) &= U_{\rm L}(t)\sqrt{\frac{Z_{\rm L}}{R_{\rm s}\Lambda^2}}\\ &\approx \pi qe\frac{\sqrt{Z_{\rm L}R_{\rm s}\Lambda^2}}{Q}f_0{\rm e}^{-t/\tau}\cos(2\pi f_0t)\\ &= 2\pi qe\frac{f_0Z_{\rm P}}{Q}{\rm e}^{-t/\tau}\cos(2\pi f_0t). \qquad (14)\end{aligned}$$

The resonator oscillates with resonant frequency f_0 and a decay rate $1/\tau$. The initial output voltage amplitude is proportional to $2\pi f_0Z_{\rm P}/Q$, hence it depends only on the physical geometry of the resonator.

If considering K passages of the circulating particle with the revolution period $T_{\rm r}$ through the resonator, the output voltage is

$$V_K(t)=\sum_{i=0}^{K-1}V(t-{\rm i}T_{\rm r}). \qquad (15)$$

For the resonance particle with revolution frequency $f_{\rm r}=f_0/m$, the phase difference between the nearest two passages is $2\pi m$, so the amplitudes add up coherently. After an infinite number of passages the output voltage goes to the equilibrium amplitude which varies between

$$\frac{2\pi qef_0Z_{\rm P}}{Q}\frac{1}{1-{\rm e}^{T_{\rm r}/\tau}}$$

shortly after a new passage and

$$\frac{2\pi qef_0Z_{\rm P}}{Q}\frac{{\rm e}^{T_{\rm r}/\tau}}{1-{\rm e}^{T_{\rm r}/\tau}}$$

before the next passage. For the off-resonance particle with $f_{\rm r}\neq f_0/m$, the phase difference between the nearest two passages is not the times of 2π, the amplitude is suppressed.

In the frequency domain, the output voltage spectrum of K passages is simply written as

$$\tilde{V}_K(f)=\tilde{I}_K(f)Z(f)\sqrt{\frac{Z_{\rm L}}{R_{\rm s}\Lambda^2}}, \qquad (16)$$

where $\tilde{I}_K(f)$ is the Fourier transform of the beam current

$$I_K(t) = qe\sum_{i=0}^{K-1}\delta(t-iT_{\rm r}).$$

4 Characteristics of the eigenmode TM$_{010}$

When charged particles pass through the resonator, the induced energy loss ΔW into the cavity mode TM$_{010}$ is

$$\Delta W \propto \frac{f_0 R_{\rm s} \Lambda^2}{Q}. \tag{17}$$

Therefore the resonant frequency f_0, quality factor Q, shunt impedance $R_{\rm s}$ and transit time factor Λ are the important characteristics of the resonator. Λ depends on the particle velocity and is related to the electric field by the following formula [9]

$$\Lambda = \frac{\left|\int_0^l E_z {\rm e}^{j\frac{2\pi f_0 z}{\beta c}}\,{\rm d}z\right|}{\int_0^l E_z\,{\rm d}z}, \tag{18}$$

where β is the relativistic factor, E_z is the electric field along the beam direction and l is the effective length of the electric field.

4.1 Estimation of the characteristics

The calculation of the characteristics is done by the software MAFIA 4 [10]. The model structure consists of a cylindrical resonator and cylindrical beam pipes on both ends, which are made of copper. A ceramic gap in the shape of a ring is located inside the resonator and the support of the ceramic gap is made of steel. All boundary conditions are electric planes.

The resonant frequency f_0 is directly calculated by the eigenmode solver, and then by applying the post processor the electric field E_z, the stored energy W, the power loss P and the accelerating voltage $V_{\rm acc}$ are calculated. The quality factor Q is derived by $Q = 2\pi f_0 P/W$ and the shunt impedance $R_{\rm s}$ is got from $R_{\rm s} = (\int_0^l E_z, {\rm d}z)^2/P$. The transit time factor Λ is calculated by inserting $V_{\rm acc}$ and E_z into the formula (18). The simulated electric field strength is plotted in Fig. 2(a). Fig. 2(b) shows the variation of the transit time factor Λ with the relativistic factor β.

4.2 Measurements of the characteristics

The resonant frequency f_0 and quality factor Q are easy to measure using a network analyzer. To measure the ratio $R_{\rm s}/Q$, a ceramic rod perturbation method is used [11], based on the relation

$$\frac{\Delta f}{f_0} = \frac{\Delta W}{W_0}, \tag{19}$$

where Δf is the frequency shift due to the perturbation, W_0 is the stored energy in the empty resonator and ΔW is the energy change. The ceramic rod must be so thin that the electric field strength at the location of the rod will not significantly change. The length of the ceramic rod must be longer than the extension of the electric field strength into the beam pipe. If such a ceramic rod is put along the particle path, $R_{\rm s}/Q$ can be derived from the following formula by measuring the resonant frequency shift,

$$\frac{R_{\rm s}}{Q} = \frac{8}{\pi^2}\frac{l}{d^2}\frac{1}{\epsilon_0(\epsilon_{\rm r}-1)}\frac{\Delta f}{f_0^2}, \tag{20}$$

where d is the diameter of the rod, l is the length of the rod and $\epsilon_{\rm r}$ is the relative permittivity, in our case $\epsilon_{\rm r} = 9.7$. The measurement results of resonant mode TM$_{010}$ are shown in Table 1, the simulated results are also summarized here for comparison.

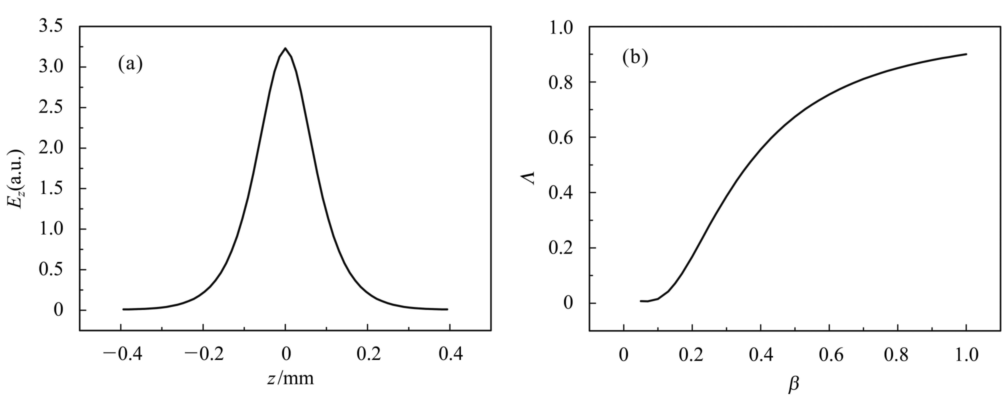

Fig. 2. (a) The calculated electric field of eigenmode TM$_{010}$. (b) The simulated transit time factor Λ versus relativistic factor β.

Table 1. MAFIA simulated and measured results of the characteristics of mode TM_{010}.

characteristics	measurements	MAFIA simulation
f_0/MHz	243.2	245.9
unloaded Q	1072	1183
$(R_s/Q)/\Omega$	71.1	68.1
R_s/kΩ	76.2	80.6

To measure the electric field along the particle path, a small copper cylinder with length $l = 22$ mm, outer radius r_o = 0.6 mm and inner radius r_i = 0.25 mm is pulled across the particle path with a step size of 20 mm. The electric field strength is derived from the frequency shift. However, it is complicated to calculate for the metallic cylinder perturbation. For an approximation the cylinder is equivalent to an ellipsoid revolution with semi-major axis a and semi-minor axis $b = r_o$ by keeping their volumes equal, thus by defining $\zeta = b/a$ the perturbation can be written as [12]

$$-\frac{(2f_0+\Delta f)\Delta f}{f_0^2} = \frac{2E_z^2(1-\zeta^2)^{3/2}\dfrac{4\pi}{3}a^3}{\ln\dfrac{1+\sqrt{1-\zeta^2}}{1-\sqrt{1-\zeta^2}}-2\sqrt{1-\zeta^2}} = cE_z^2,$$

$$c = \frac{2(1-\zeta^2)^{3/2}\dfrac{4\pi}{3}a^3}{\ln\dfrac{1+\sqrt{1-\zeta^2}}{1-\sqrt{1-\zeta^2}}-2\sqrt{1-\zeta^2}}. \tag{21}$$

Since the thickness of the cylinder is much greater than the skin depth, the hollow inside of the cylinder is field free. Let the semi-minor axis b of ellipsoid be equal to the outer radius of the cylinder,

$$\frac{4\pi}{3}b^2a = \pi r_o^2 l. \tag{22}$$

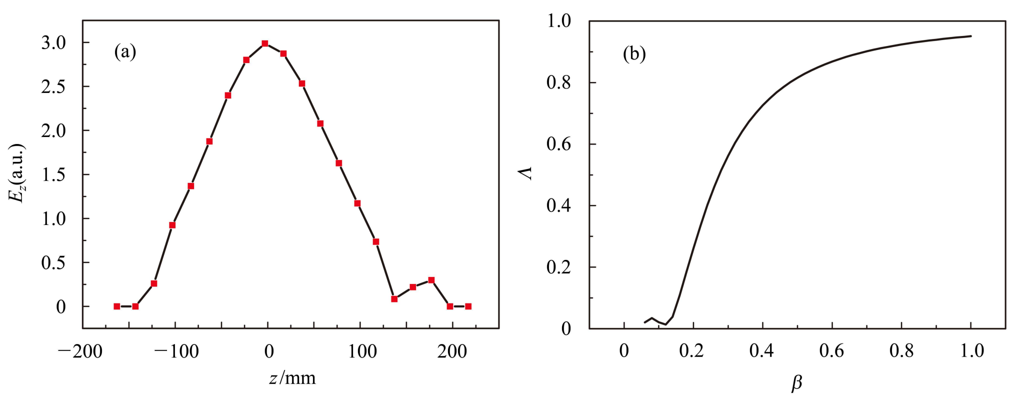

Fig. 3. Measured electric field and transit time factor of eigenmode TM_{010}

Therefore $a = \frac{3}{4}l = 16.5$ mm, $\zeta = \frac{0.6\ \text{mm}}{16.5\ \text{mm}} = 0.037$, $c = 3.14\times10^{-6}$ m^{-3}. By then the electric field is calculated from Eq. (21) by inserting the measured value of resonant frequencies, which is shown in Fig. 3(a). Furthermore the transit time factor Λ can be easily derived by inserting the electric field result into Eq. (18), shown in Fig. 3(b). From the curve it is inferred that the resonant pickup is more sensitive to the high energy beam.

5 Conclusions

The measurements of characteristics are in good agreement with the simulation. Therefore, the resonator is well designed. With a shunt impedance of 76 kΩ the resonant Schottky pickup will work as a highly sensitive detector to detect the signals of even single ions. The sensitivity of the Schottky pickup system is limited by noise background, which is generated in the Schottky pickup and electronics. Although all of the components generate noise, only the pickup and the first stage amplifier are important for the signal to noise ratio. The noise from the resistive wall and the lossy dielectrics of the resonant pickup exhibit a noise temperature T_p of about 298 K, the noise power density at the resonant frequency can be described as $n_p = k_B{\cdot}T_p$, where k_B is Boltzmann's constant. The equivalent input noise power density of the first amplifier is described by the noise figure $F = 0.7$ dB, $n_a = k_B \cdot 290K \cdot (F-1)$. Therefore the total noise power density from the output of the pickup at the resonant frequency is $n_p + n_a \approx -173$ dBm/Hz. On the other hand, the output signal power density P_s of a single ion can be estimated by $P_s = 1/4(qef_r)^2R_s\Lambda^2/(m\delta f)$. As an example it is assumed that a beam of the energy of

368 MeV/u and the relative Schottky band width $\delta f/(f_{\rm r}) \approx 10^{-7}$, thus a single ion of charge state $q \geqslant 30$ can be detected with a signal to noise ratio of above 5:1. However the actual signal to noise ratio may be somewhat worse since the environment interference would make a contribution to the background noise.

The resonant Schottky pickup will be installed in the storage ring CSRe for the first measurements. The signal extracted from the coupling loop will be amplified by an amplifier chain including a low-noise amplifier and two broad-band amplifiers and then sampled with a real-time spectrum analyzer. Furthermore a special recorder is planned to be added to the spectrum analyzer for high-speed and long-duration recording of raw data. The stored data can be off-line analyzed to get the power spectrum. With such a measurement system, nuclear masses and lifetimes can be measured under electron cooling at CSRe.

References

1 Bertulani C A. Nucl. Phys. A, 1997, **626**: 187c–198c

2 Litvinov Yu A et al. Acta Physica Polonica B, 2010, **41**: 511–523

3 Bosch F. J. Phys. B: At. Mol. Opt. Phys., 2003, **36**: 585–597

4 XU H S et al. Chin. Sci. Bull, 2009, **54**: 4749

5 Ohtsubo T et al. Phys. Rev. Lett., 2005, **95**: 052501

6 Radon T et al. Phys. Rev. Lett., 1997, **78**: 4701

7 Lambertson Glen R. electromagnetic detectors. In: Month M and Turner S ed. lecture notes in physics, vol.343. Berlin, Heidelberg: Springer-Verlag, 1989, 380

8 Goldberg D A et al. AIP Conf. Proc., 1992, **249**: 537

9 Duff J Le. High frequency non-ferrite cavities. In: Miles J. CERN Accelarator School on redio frequency engineering. Geneva: CERN, 2005. 50–57

10 MAFIA version 4.0. CST GmbH, Germany. http://www.cst-china.cn/CST2009/product/mafia

11 Carter R G. Microwave theory and techniques, IEEE Trans., 2001, **49**(5): 918

12 Majer L C et al. Journal of Applied Physics, 1952, **23**(1): 68